Study on Direct Torque Control Methods of a Doubly Fed Induction Machine Working as a Stand-Alone DC Voltage Generator

Paweł Maciejewski and Grzegorz Iwanski, *Senior Member, IEEE*

***Abstract*—The article presents a comparison of different Direct Torque Control methods of a Stand-Alone Doubly Fed Induction DC-Voltage Generator, with classic field oriented control used as a benchmark. The system consists of a doubly fed induction generator the stator circuit of which is connected to the DC-bus with a diode rectifier, and the rotor circuit converter is connected to the same DC bus. The main problem of this power generation system are large torque oscillations caused by a nonlinear diode rectifier connected to the stator. Three direct torque control algorithms are described as a means of reduction of this drawback with simultaneous control of DC bus voltage and stator voltage frequency. The methods differ by the second variable used for control in parallel to the torque control path. The selected second variable is the *d* component of the rotor current vector, the *d* component of the stator flux or the stator flux module.**

***Index Terms*—Autonomous power source, DC generator, direct torque control, doubly fed induction generator (DFIG).**

I. Introduction

THE main application of a doubly fed induction machine DFIG is AC power generation [1]. However, recently its use for DC voltage generation has been intensively studied [2]–[6]. The main focus is on DC micro grid [2], [3] as well as autonomous operation with DC output [4], [5]. Like in AC systems, here its main advantage is the reduced size of the power converter and frequency stabilization despite variable rotor speed. Autonomous operation of DFIG for AC power generation has been studied in recent years [7]–[9]. In the case of nonlinear load, electromagnetic torque T_{em} pulsations occur. Similarly, in the case of the DFIG-DC system described in the paper, torque pulsations may be significant due to the nonlinear character of the diode rectifier. They can be eliminated with various techniques such as resonant controllers [3] and active filtration [2].

In AC stand-alone operation, the goal is to regulate stator voltage and frequency independently of the load condition. The most popular control approaches are amplitude-angle regulation and field oriented control (FOC) [7]–[10]. Recently direct torque control (DTC) for autonomous DFIG has been developed [11], [12]. This control method allows simple and effective torque pulsation reduction in the DFIG-DC power generation system. For an AC system, torque stabilization during unbalanced and nonlinear load feeding has no justification due to the main goal, which is high quality symmetrical sinusoidal stator voltage. In contrast, in the DFIG-DC system, torque oscillations cancellation can be applied, as the stator voltage shape is less important, because it is not directly used for other load supply.

The previously proposed solutions for the DFIG-DC system have some drawbacks. In the method proposed by *Marques* [3] resonant controllers have been implemented, for which the anti-windup structures are not trivial. To achieve satisfactory torque pulsation reduction, a large number of those oscillatory terms operating in parallel have to be implemented. It causes problems with proper tuning of such a controller composed of several dynamic terms operating in parallel. Furthermore, even slight frequency changes in dynamic states cause that the oscillatory terms resonant frequency must be adapted. *Yu* [13] suggests using an active filtering function of the load side converter. This solution increases the cost of the system and can be justified when, besides feeding the three-phase rectifier, the stator of the machine supplies directly other loads requiring high quality stator voltage. In the DFIG-DC system operating without an additional AC load connected to the stator terminals, the use of the second power converter is questionable. In [12] *Gundavarapu* proposed DTC control for DFIG-DC with the use of a switching table and histeresis controllers. This is similar to DTC control proposed in [14], well documented in literature. This type of control produces high torque pulsations and has variable switching frequency. Moreover, in case of autonomous systems, precise frequency control is difficult to achieve. The method proposed by *Marques* in [15] based on finite state predictive control also involves the difficulty of complex stator freqency control, but due to predictive control, which is fast, torque pulsations are insignificant.

This paper presents a comparison of three direct torque control methods with PWM modulation for a stand-alone DC voltage generation DFIG system. A model of the machine is presented in Section II. Section III outlines field oriented control FOC as a background to the proposed and tested DTC methods. The DTC methods are presented in sections IV-VI. Section VII describes instantaneous power *p* component waveforms influencing the dc

Manuscript received January 31, 2020; revised April 29, 2020 and July 16, 2020; accepted July 26, 2020. Date of publication July 29, 2020; date of current version May 21, 2021. *(Corresponding author: Grzegorz Iwanski.)*

The authors are with the Institute of Control and Industrial Electronics, Warsaw University of Technology, 00-662 Warszawa, Poland (e-mail: pawel.maciejewski@ee.pw.edu.pl; iwanskig@isep.pw.edu.pl).

Color versions of one or more of the figures in this article are available online at https://ieeexplore.ieee.org.

Digital Object Identifier 10.1109/TEC.2020.3012589

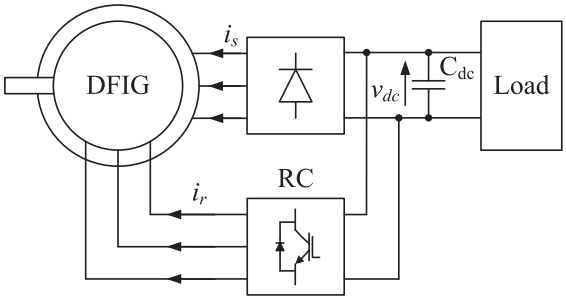

Fig. 1. Scheme of the stand-alone DC voltage generator with a doubly fed induction generator.

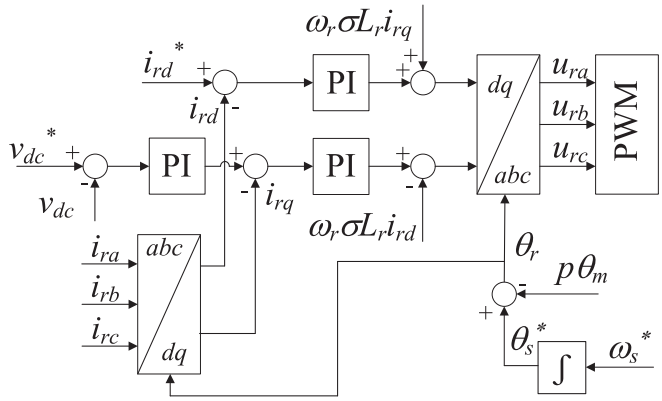

Fig. 2. Scheme of field oriented control for the DFIG-DC system.

bus voltage, whereas Section VIII and IX describe simulation and experimental tests results.

II. System Description and Modeling

The analyzed system shown in Fig. 1 consists of a doubly fed induction machine connected to the DC-bus with a diode rectifier on the stator side. The rotor of the machine is fed by a power converter connected to the DC-bus.

Standard equations of the machine are used for the control synthesis.

$$v_s = R_s\, i_s + \frac{d}{dt}\psi_s + j\omega_s\psi_s \tag{1}$$

$$v_r = R_r\, i_r + \frac{d}{dt}\psi_r + j\left(\omega_s - p\omega_m\right)\psi_r \tag{2}$$

$$\psi_s = L_s\, i_s + L_m i_r \tag{3}$$

$$\psi_r = L_r\, i_r + L_m i_s \tag{4}$$

$$T_e = \frac{3}{2}\, pL_m\left(i_{rd}i_{sq} - i_{rq}i_{sd}\right) \tag{5a}$$

$$T_e = \frac{3}{2}\, p\frac{L_m}{L_s}\left(\psi_{sq}i_{rd} - \psi_{sd}i_{rq}\right) \tag{5b}$$

$$C_{dc}\,\frac{dv_{dc}}{dt} = -i_{sq} + i_L \tag{6}$$

in which ψ_r – rotor flux, ψ_s – stator flux, T_{em} – electromagnetic torque, p – pole pairs, L_m – magnetizing inductance, L_r – rotor inductance, L_s – stator inductance, $\sigma = 1 - \frac{L_m^2}{L_r L_s}$, C_{dc} – dc bus capacity, i_L – load current, v_r, v_s – rotor and stator voltage, v_{dc} – dc voltage, R_r, R_s – rotor and stator resistance.

Stator voltage frequency control methods can be divided into two groups: with open loop frequency control and with closed loop frequency control. In open loop frequency control the frequency of stator voltage is set arbitrarily by reference angular speed of coordinates frame and the transformation angle is calculated as a difference between reference angle (integrated angular speed) and rotor position [16]. This is the simplest way used, e.g., in field oriented control FOC. Another way of stator frequency regulation relies on stator flux vector module regulation. The absolute value of the first harmonic of electromotive force is represented by (7).

$$|E_s| = \omega_s\ |\psi_s| \tag{7}$$

It can be deduced that for constant stator voltage (so the stator electromotive force if stator resistance voltage drop is neglected), frequency of stator voltage can be set by a change of the stator flux vector module [4]–[12]. A possible inaccuracy may occur, caused by inadequate flux reference to the desired stator voltage pulsation. The inaccuracy can be compensated for by a superior controller of stator voltage pulsation if necessary.

III. Field Oriented Control of the DFIG-DC System

The FOC control method described in [7] is an example of a method with open loop frequency control. This control system is composed of rotor current vector components in the *dq* reference frame as presented in Fig. 2. The reference *d* current vector component is set on the magnetizing current level. The *q* vector current component is set by a DC voltage regulator. This ensures orientation of the reference frame along the stator flux space vector. The demanded value of magnetizing current can be measured or estimated on the basis of the machine parameters. This method (FOC) as the most frequently published method for the DFIG-DC system will be used as a reference for comparison of torque pulsations in this paper.

IV. Direct Torque and Rotor Current Vector d Component Control - $\mathrm{DTI_dC}$

In the DFIG-DC system one of the desired properties is reduction of torque pulsations. This can be achieved by direct torque control [11]. As described in Section II, pulsation can be controlled by controlling stator flux or rotor slip. This is an equivalent approach to slip angle control described in literature [17]. In the proposed direct control methods with open loop frequency control, one regulator is responsible for torque control, whereas the second one for controlling the machine magnetization. The voltage pulsation is achieved by setting an arbitrary rotor reference frame transformation angle.

The direct torque and rotor current *d* component control $\mathrm{DTI_dC}$ presented in Fig. 3 consists of a *d* rotor current vector component regulator and a torque regulator.

As far as the first term in parentheses of equation (5b) is at a negligible level, we can derive that $T_e \sim i_{rq}$. This occurs in

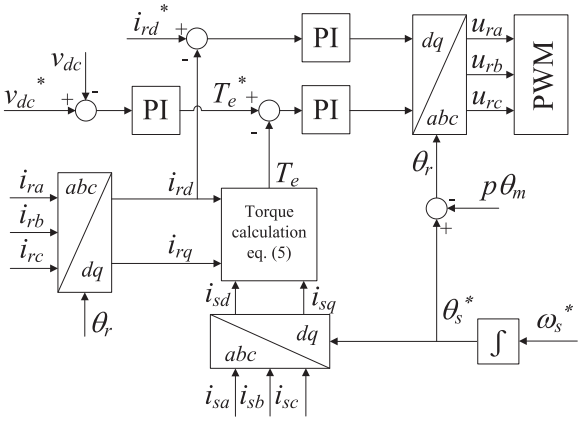

Fig. 3. Scheme of the DTI$_{\mathrm{d}}$C control method for the DFIG-DC system.

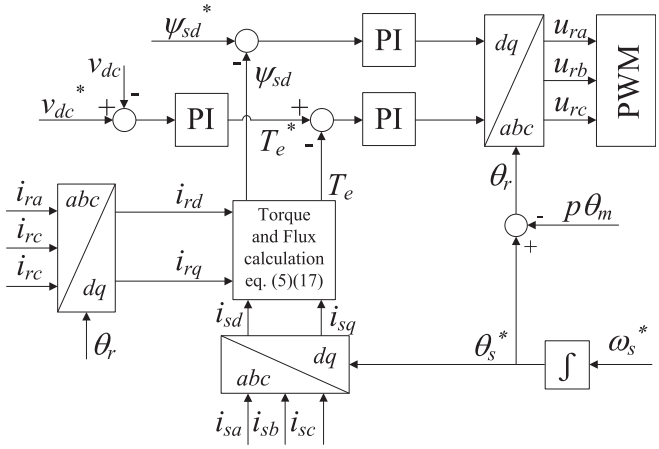

Fig. 4. Scheme of the DTψ_{d}C method for the DFIG-DC system.

two situations. The first one is for ideal orientation of reference frame with flux ($\psi_{sq} = 0$), and second one is for ($i_{rd} = 0$). The product of both components $\psi_{sq} i_{rd}$ shows that this term in (5b) is incomparably smaller than the main component $\psi_{sd} i_{rq}$ not only in these two cases, but in a relatively wide range of reference frame positions. Thus, from the torque control path point of view, precise orientation of the reference frame along the stator flux vector is not necessarily the most important, whereas as it will be shown in the simulation results section, referencing i_{rd} close to zero can be interesting and may be an inspiration for future research.

Regardless of which manner has been chosen – reference *d* component of the rotor current vector at the magnetizing current level giving ψ_{sq} close to zero, or $i_{rd} = 0$, equation (5b) simplifies. From (4) and simplified (5b) v_{rq} as a function of electromagnetic torque can be derived:

$$v_{rq} = -\frac{2L_s}{3\psi_{sd} p L_m}\left(R_r T_e + \sigma L_r \frac{d}{dt} T_e\right) + \omega_r \psi_{rd} \tag{8}$$

It can be described using the following transfer function:

$$\frac{T_e}{v_{rq}}(s) = \frac{A}{s\sigma L_r + R_r} \tag{9}$$

$$A = -\frac{3\psi_{sd} p L_m}{2L_s} \tag{10}$$

The torque reference is given by a DC voltage regulator. From equations (5b) and (6), the following can be derived with the assumption of no load conditions and orientation of the reference frame with the stator flux vector:

$$\frac{dv_{dc}}{dt} = -\frac{2}{3}\frac{1}{\psi_{sd} p C_{dc}} T_e \tag{11}$$

The above equation can be described using the following transfer function:

$$\frac{v_{dc}}{T_e}(s) = \frac{1}{sB} \tag{12}$$

$$B = -\frac{3}{2}\psi_{sd} p C_{dc} \tag{13}$$

In order to derive the transfer function for control of the rotor current vector *d* component, a full model of disturbances and decoupling terms is introduced. It is obtained by inclusion of the stator voltage equation (1) and flux equations (3), (4) in the rotor voltage equation (2). Thus, the full model of the control plant, stator voltage disturbance and couplings between control paths is given by:

$$v_{rd} = R_r i_{rd} + \sigma L_r \frac{d}{dt} i_{rd} + \frac{L_m}{L_s}\left(v_{sd} - R_s i_{sd}\right) + \omega_s \psi_{sq} - \left(\omega_s - p\omega_m\right)\psi_{rq}. \tag{14}$$

Assuming for the case of ψ_{sq} close to zero, (14) can even be simplified to:

$$v_{rd} = R_r i_{rd} + \sigma L_r \frac{d}{dt} i_{rd} - \left(\omega_s - p\omega_m\right)\psi_{rq}. \tag{15}$$

In both cases the control plant can be described using the following transfer function:

$$\frac{i_{rd}}{v_{rd}}(s) = \frac{1}{s\sigma L_r + R_r} \tag{16}$$

V. Direct Torque and Stator Flux Vector d Component Control - DTψ_{d}C

The direct torque and stator flux *d* component control DTψ_{d}C method presented in Fig. 4 consists of a stator flux vector *d* component regulator and a torque regulator. The reference torque signal is given by a DC voltage regulator. In stand-alone DFIG systems, the machine should be kept magnetized at no load conditions. This involves supplying a sufficient value of magnetizing current on the rotor side, in order to maintain constant voltage on the stator terminals despite lack of DC load.

The reference flux vector *d* component is assumed to be equal to its length and is calculated on the basis of the requested magnetization current at no load conditions

$$\psi_{sd}^{*} = \left|\psi_s^{*}\right| = \left|i_m\right| L_s, \tag{17}$$

whereas the actual value of the flux vector ψ_{sd} component is calculated after decomposition of (3) to the *dq* components.

$$\psi_{sd} = L_s\, i_{sd} + L_m i_{rd}. \tag{18}$$

The v_{rd} equation can be derived from (2)-(4) after decomposition to orthogonal *dq* components.

$$v_{rd} = \frac{R_r}{L_m}\,\psi_{sd} + \frac{L_r}{L_m}\frac{d}{dt}\psi_{sd} - \omega_r \psi_{rq} \tag{19}$$

The above equation can be described using the following transfer function:

$$\frac{\psi_{sd}}{v_{rd}}(s) = \frac{L_m}{sL_r + R_r} \tag{20}$$

The transfer function for the DC bus voltage and torque control path is the same as described by (10)-(15) because the same equations are used for linear model derivation.

It has to be noted that in the presented field oriented control method (Fig. 2), and both direct torque control methods (Fig. 3 and Fig. 4) with the arbitrary referenced *d* component of rotor current vector or the *d* component of stator flux vector, respectively, precise orientation of the reference frame along stator flux vector is not reached without extra structures modifying *d* axis commanded variables. Slight phase shift between frame orientation and stator flux orientation does not cause considerable problems, which will be shown in Section VII presenting simulation results of the DFIG-DC system with the 2MW DFIG model.

VI. Direct Torque and Stator Flux Vector Module Control - DT|ψ|C

Lack of precise orientation of the frame in the previously discussed methods does not cause stator frequency deviation, but only phase displacement between the reference frame and the stator flux vector. Conversely, in the classic direct torque and flux module control DT|ψ|C presented in this section, the synchronization structure is obligatory, when stator frequency stabilization is requested. The synchronization structure can be made in different manners, whereas all of them are used for modification of the flux reference module.

In [12] the authors proposed a DTC method with closed loop frequency control with hysteresis torque and flux controllers. This type of inner controllers results in significant torque pulsations and variable switching frequency depending on the width of hysteresis and algorithm sampling frequency [6]. Switching frequency torque pulsations resulting in this control method can be greater than those caused by a stator connected diode rectifier [12]. It questions the justification of the use of hysteresis controllers.

The direct torque and stator flux module control DT|Ψ|C method is presented in Fig. 5. The main difference between this control method and the previous methods is the way of transformation angle calculation. In DT|Ψ|C the slip angle for transformation is the result of the stator flux angle and mechanical angle subtraction. This is a similar approach to the classic DTC method described in literature [14]. In contrast to DTΨ$_{\mathrm{d}}$C, in the *d* axis the stator flux module is controlled. The

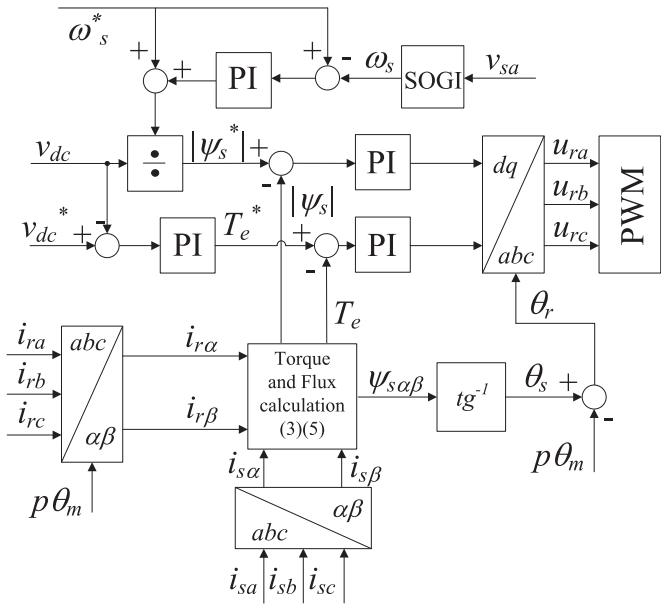

Fig. 5. Scheme of the DT|ψ|C control for the DFIG-DC system.

transformation angle is calculated as the difference between the actual stator flux angle and mechanical angle.

Due to inaccuracy of flux reference determination (flux vector average length changes depending on the stator current and stator voltage shape), stator voltage frequency may differ from the reference value. To compensate for this difference a stator frequency outer controller (corrector) is implemented in the proposed control method. The actual stator voltage pulsation ω_s is determined using second order generalized integrator (SOGI).

VII. Discussion on the Instantaneous Power p Component

DC voltage oscillations are directly generated by the instantaneous *p* component of power flowing to the DC circuit. This power is the sum of stator p_s and rotor p_r power. The average value of the *p* component of power is definitional active power. Electromagnetic power (calculated as a product of electromagnetic torque and mechanical speed) reduced by the power of losses on the stator and rotor resistances gives total active power as a sum or stator and rotor active powers (21) responsible for energy delivery to the DC bus.

$$\begin{aligned} &T_{e\_avg}\omega_m - R_s\left(i^2_{sa\_rms} + i^2_{sb\_rms} + i^2_{sc\_rms}\right) \\ &\quad - R_r\left(i^2_{ra\_rms} + i^2_{rb\_rms} + i^2_{rc\_rms}\right) = P_s + P_r \end{aligned} \tag{21}$$

The same cannot be derived for instantaneous power p_s and p_r. It could be derived for the constant flux vector, such as in a DFIG-AC system with sinusoidal stator voltage (so constant stator flux), but not in the analyzed DFIG-DC system, in which the nonlinear character of the diode rectifier causes nearly six step voltage on the stator side, and, consequently, flux changes. It means that instantaneously energy is not taken only from the electromechanical conversion, but also from demagnetization of the machine (when equivalent flux vector decreases), and in another point, not whole mechanical energy conversion is

delivered to the DC circuit through stator and rotor side, but part of this energy is used for magnetization increase (when equivalent flux vector increases).

The instantaneous power equation is given by (22)

$$T_e\omega_m - \frac{3}{2}R_s\left(i_{sd}^2+i_{sq}^2\right) - \frac{3}{2}R_r\left(i_{rd}^2+i_{rq}^2\right) - p_{\Delta\psi} = p_s + p_r \tag{22}$$

whereas $p_{\Delta\psi}$ is the instantaneous power responsible for field changes, the average value $P_{\Delta\psi}$ of which equals zero. The instantaneous value can be calculated in the following way, as the magnetizing and leakage inductances energy changes $\frac{dE_L}{dt}$.

$$p_{\Delta\psi} = \frac{dE_{L_{\sigma s}}}{dt} + \frac{dE_{L_{\sigma r}}}{dt} + \frac{dE_{L_m}}{dt} \tag{23}$$

which can be further derived as

$$p_{\Delta\psi} = \frac{3}{2}\left(\frac{L_{\sigma s}}{2}\frac{d\left(i_{sd}^2+i_{sq}^2\right)}{dt} + \frac{L_{\sigma r}}{2}\frac{d\left(i_{rd}^2+i_{rq}^2\right)}{dt} + \frac{L_m}{2}\frac{d\left(\left(i_{sd}+i_{rd}\right)^2+\left(i_{sq}+i_{rq}\right)^2\right)}{dt}\right)$$

$$= \frac{3}{2}\left(\frac{L_s}{2}\frac{d\left(i_{sd}^2+i_{sq}^2\right)}{dt} + \frac{L_r}{2}\frac{d\left(i_{rd}^2+i_{rq}^2\right)}{dt} + L_m\frac{d\left(i_{sd}i_{rd}+i_{sq}i_{rq}\right)}{dt}\right)$$

$$= \frac{3}{2}\left(\frac{L_s}{2}\frac{d\left(|i_s|^2\right)}{dt} + \frac{L_r}{2}\frac{d\left(|i_r|^2\right)}{dt} + L_m\frac{d\left(i_s\cdot i_r\right)}{dt}\right), \tag{24}$$

in which $i_s \cdot i_r$ is a dot product of stator and rotor current vectors.

Depending on the control method, torque pulsations differ, and the sum of instantaneous stator p_s and rotor p_r power will differ as well. The waveform of this summarized power does not correspond to the waveforms of electromagnetic torque as the oscillations characters are different. Simulation results of electromagnetic power calculated as $T_e\omega_m$, sum of instantaneous stator and rotor power $(p_s + p_r)$, instantaneous power of losses on stator and rotor resistances (p_{loss}), and instantaneous power represented stator and rotor flux changes $(p_{\Delta\psi})$ are shown in Fig. 6.

VIII. Comparison of Simulation Results

Simulation tests are provided for the 2MW DFIG model, as for this range it is economically and technically justified. Machine parameters are shown in the appendix (Tab. III). Fig. 7 presents the simulation results of two FOC methods.

The first (Fig. 7a) presents a results of control structure adapted from the DFIG-AC system presented in [7] to the DFIG-DC system, through replacement of stator voltage controller by the DC bus voltage controller. The method shows precise orientation of reference frame along the stator flux vector. The second (Fig. 7b) presents a results of FOC method from Fig. 2. In this method we can observe slight phase shift of the reference frame manifested by non-zeroed q component of the stator flux vector. Despite this phase shift, the obtained results are similar, and both methods entail significant torque oscillations.

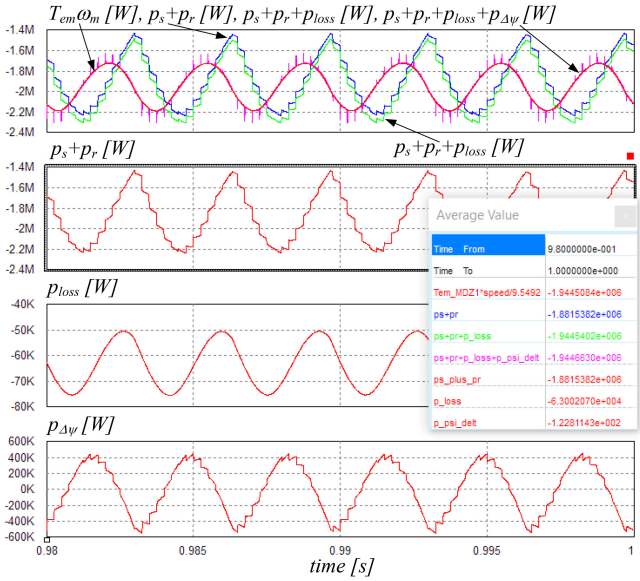

Fig. 6. Instantaneous powers waveforms in the DFIG-DC system.

Introduction of a torque controller in the q axis instead of the q component of current (DTI$_\mathrm{d}$C) provides insignificant reduction of electromagnetic torque pulsation, but visibly (about three times) reduces DC voltage oscillations (Fig. 8a). Setting the d component of current to zero, the phase shift between reference frame orientation and stator flux vector increases, but both torque and DC voltage oscillations are two times smaller than for FOC methods (Fig. 8b).

Replacement of the current regulator in the d axis by a flux regulator (DTψ_dC, DT$|\psi|$C) provides larger reduction (three times) of machine torque, independently whether the regulated variable is the d component of flux (Fig. 9a) or the flux module (Fig. 9b). For both direct torque control methods with flux regulators results are similar despite slight phase shift between the reference frame and the stator flux vector position. DC voltage ripples are at the same level as in FOC.

IX. Experimental Results

The experimental studies were conducted with DFIG connected from the stator side to a 6-pulse diode rectifier and fed on the rotor side from a 2-level converter connected to the stator side DC bus (Fig. 10). The machine is driven using a vector controlled induction motor with speed control. The control methods of the DFIG-DC system were implemented on a TMS320F28335 microcontroller. The data has been registered using a Yokogawa DL850 scope recorder. The parameters of the proportional-integral controllers in the proposed direct torque control methods are shown in Table I.

In case of the DTI$_\mathrm{d}$C method (Fig. 12), approximately 50% reduction of torque pulsation peaks comparing to FOC (Fig. 11) is achieved in the experiment. The amplitude of torque pulsation fundamental harmonic is reduced 4 times in comparison to the FOC method. The DTI$_\mathrm{d}$C method allows to control the stator frequency and voltage amplitude. In case of the DT$|\psi|$C

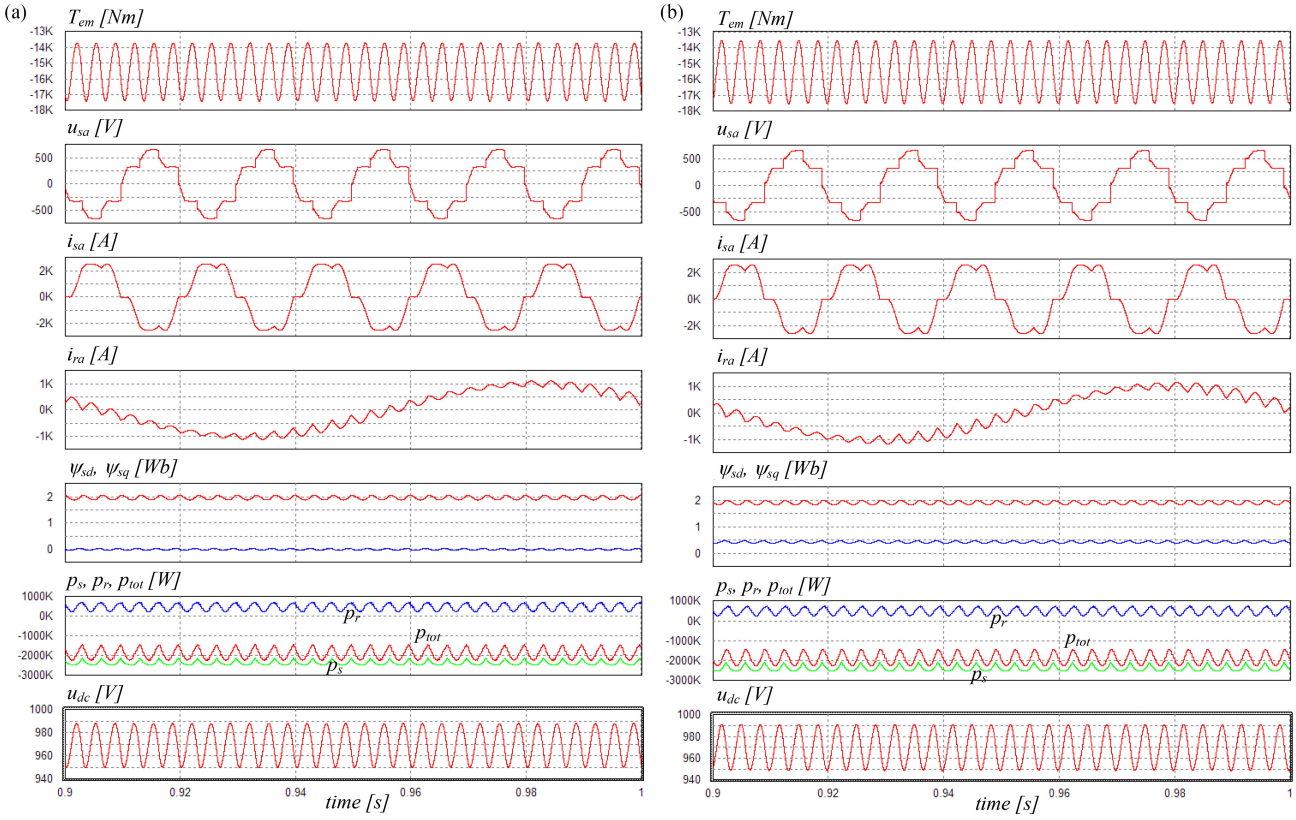

Fig. 7. Simulation results of the 2MW DFIG-DC system with FOC control methods, a) from [7] with DC voltage controller, b) from Fig. 2.

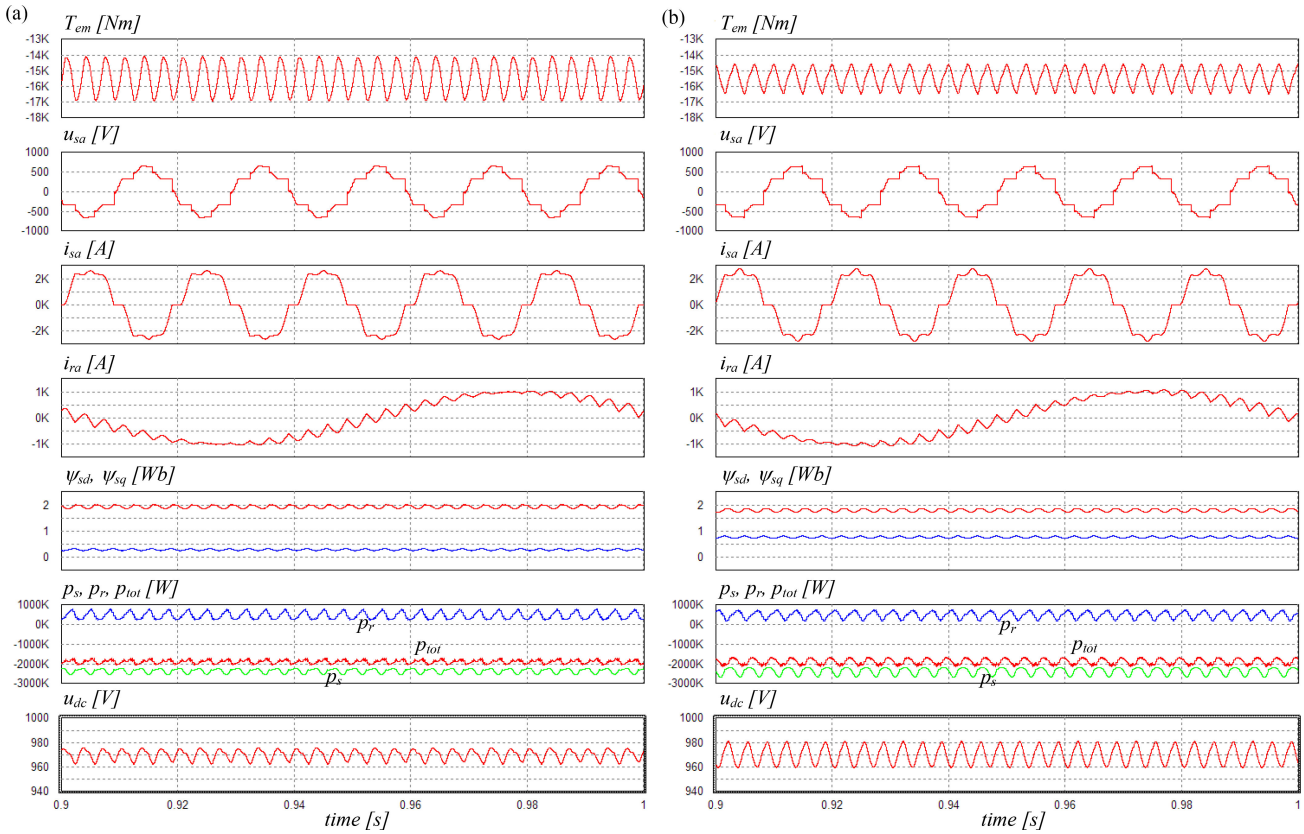

Fig. 8. Simulation results of the 2MW DFIG-DC system with $\mathrm{DTI_dC}$ control methods, a) with $i_{rd}^{*} = i_m$, b) with $i_{rd}^{*} = 0$.

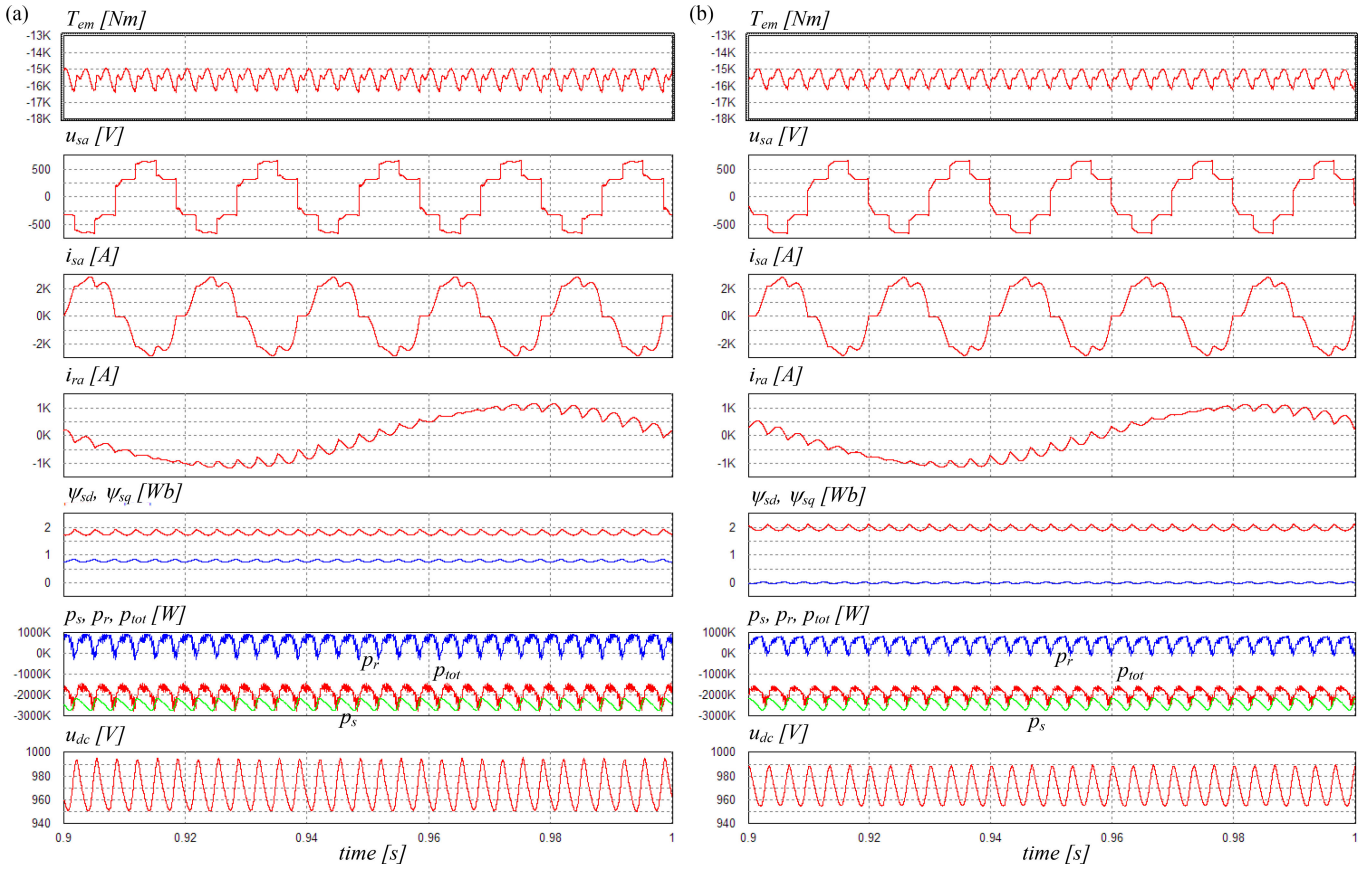

Fig. 9. Simulation results of the 2MW DFIG-DC system with direct torque and flux control, (a) DTψ_dC, (b) DT|ψ|C.

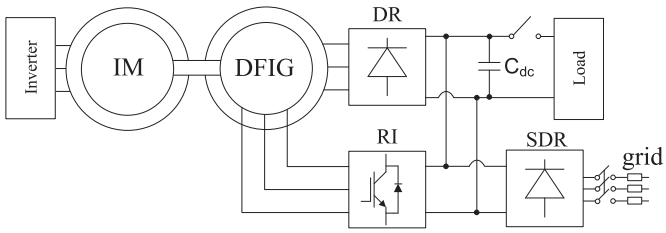

Fig. 10. Scheme of the small scale laboratory setup of the DFIG based stand-alone DC voltage generating system.

TABLE I
PI CONTROLLERS SETTINGS IN EXPERIMENT

CONTROLLER	K_p	K_i
PI_{Te}	10	33
$PI_{\|\Psi\|}$	150	40
PI_{Vdc}	5	50

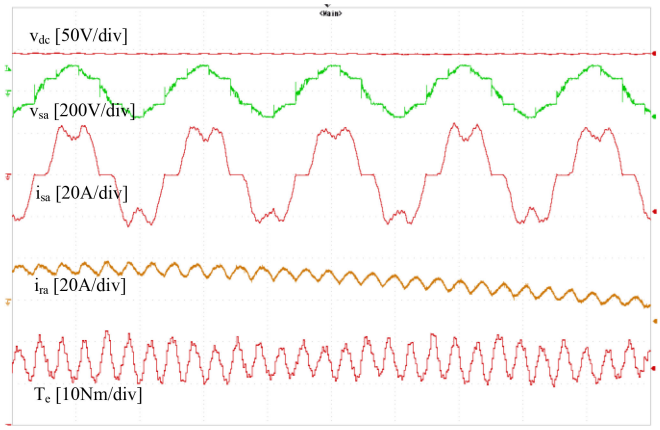

Fig. 11. Experimental results of the FOC method in steady state.

method presented in Fig. 13 further torque pulsation reduction is achieved, resulting in 70% reduction in relation to FOC. Table II provides a synthetic comparison of results obtained with the analyzed methods both in simulation and experimental tests. As the power range of simulation and experimental models differs, the absolute value of torque oscillations differs. Independently of that in both simulation and experiment, torque ripples are the smallest for direct torque and flux module control.

It can be observed that depending on the control method rotor current pulsations differ, but are not eliminated fully, because the machine flux is not constant. Possibly, like in the method discussed in [3], more exact results can be obtained with the use of oscillatory terms as regulators of torque in one axis

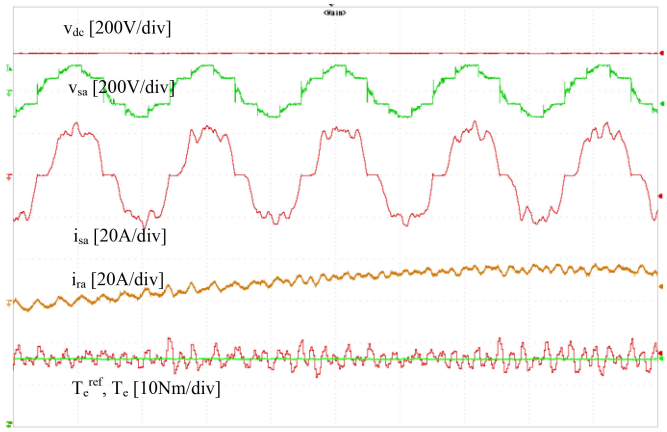

Fig. 12. Experimental results of the DTI$_d$C method in steady state.

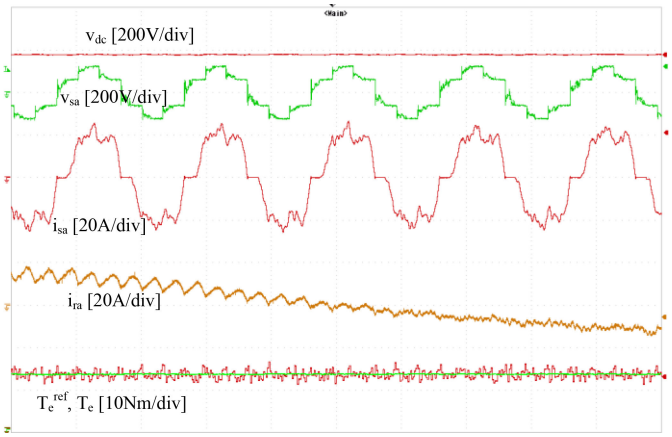

Fig. 13. Experimental results of the DT|ψ|C method in steady state.

TABLE II
COMPARISON OF TORQUE PULSATIONS OBTAINED FOR DIFFERENT METHODS IN EXPERIMENTAL AND SIMULATION RESULTS

TORQUE PULSATIONS	FOC	DTI$_d$C	DT|Ψ|C
	Experiment/Simulation		
Pulsations peak to peak value [Nm]	10/3.8k	5/3k	3/1.1k
Ratio of pulsation to mean torque value [%]	62/25	33/20	20/7
Ratio of pulsation to rated torque value [%]	20/25	9.8/20	6/7
DC voltage peak to peak oscillations [V]	-/40	-/16	-/35
Ratio of DC voltage oscillations to rated value [%]	-/4.1	-/1.5	-/3.5

and current/flux in the second axis, and keeping torque pulsations reduced the rotor current pulsation significantly. However, implementation of oscillatory terms must be very careful. They can create reference rotor voltage oscillations higher than possible in realization with the available DC voltage value for adequately matched DC voltage to the machine turns ratio. In [3] the available DC voltage is much higher than related to the stator to rotor turns ratio and assumed speed range, so the rotor converter has better abilities in the torque oscillations reduction. However, implementation of resonant terms for direct torque control methods requires further studies.

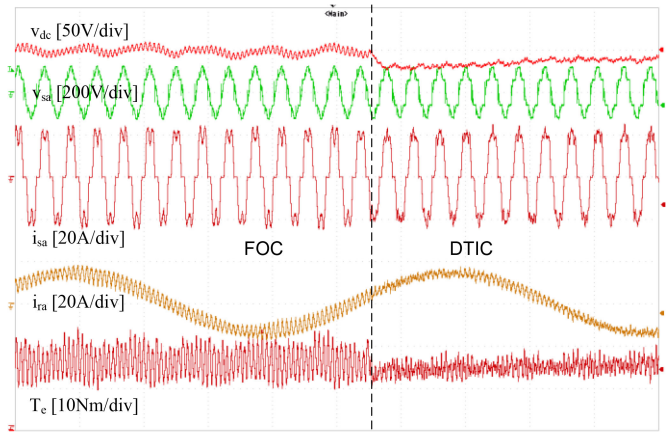

Fig. 14. Comparison of FOC and DTI$_d$C in experimental tests.

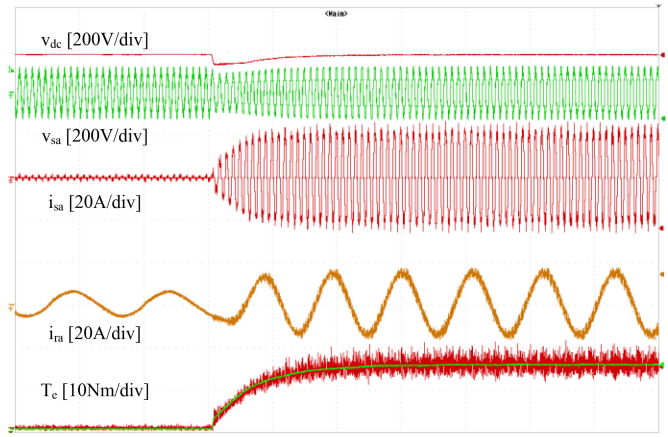

Fig. 15. Experimental results of DTI$_d$C before and after step loading.

Experimental results in Fig. 14 present a direct comparison of torque pulsation for the DTI$_d$C and FOC methods by switching between the control methods during the DFIG-DC system operation. Experimental results of step loading for the proposed control methods of DFIG-DC are shown in Fig. 15-16. Oscillograms show DC-voltage, stator voltage, stator current, rotor current and electromagnetic torque. All the proposed methods allow to maintain a reference value of DC voltage after step loading with a relatively short transient.

Short, approximately 200 ms, voltage dips occur due to voltage controller action. In case of more demanding application, dips can be shortened by applying a feed-forward load power/current signal with the use of a load current sensor.

Fig. 17-18 present step unloading and finally no-load operation for the DTI$_d$C (Fig. 17) and DT|ψ|C (Fig. 18) method. Change of the rotor current frequency after unloading can be observed due to the stator frequency controller action.

Experimental results of variable speed operation for the proposed control methods of the DFIG-DC system are shown in

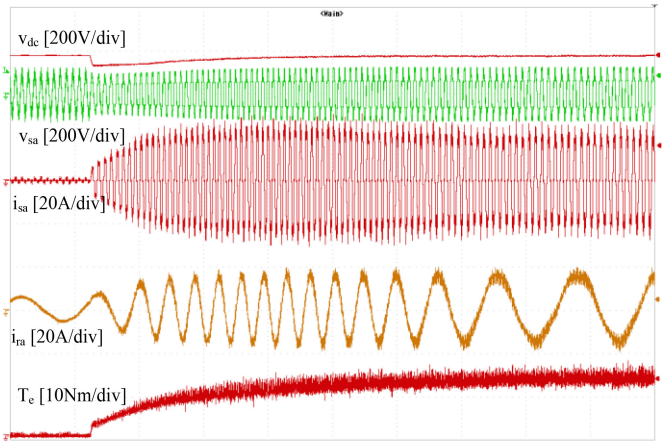

Fig. 16. Experimental results of DT|ψ|C before and after loading.

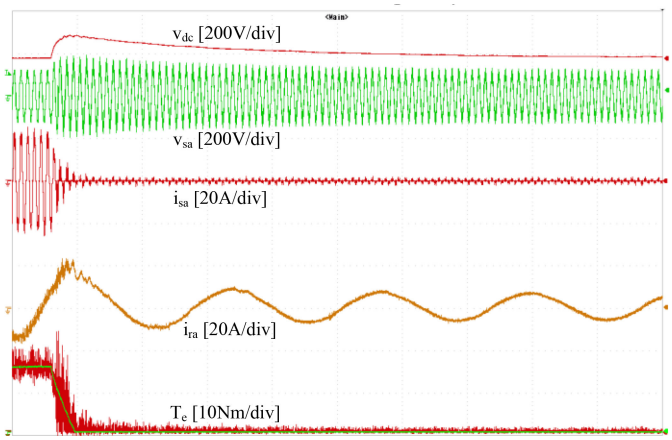

Fig. 17. Experimental results of DT|ψ|C at no load condition.

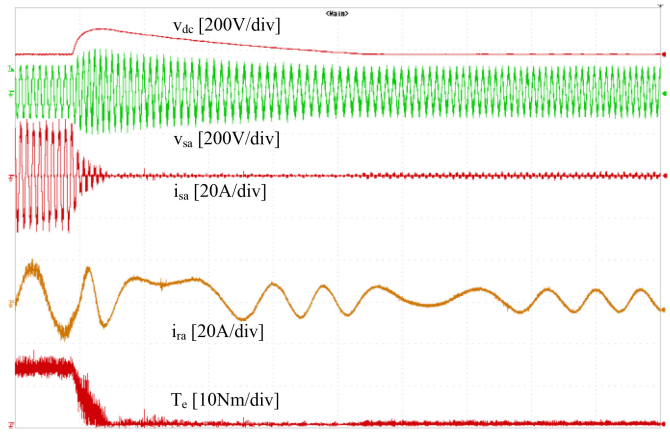

Fig. 18. Experimental results of DT|ψ|C at no load condition.

Fig. 19-20. Oscillograms show DC-voltage, stator voltage, stator current, rotor current and electromagnetic torque. All the proposed methods allow operation in sub- and super-synchronous speed region as well at synchronous speed.

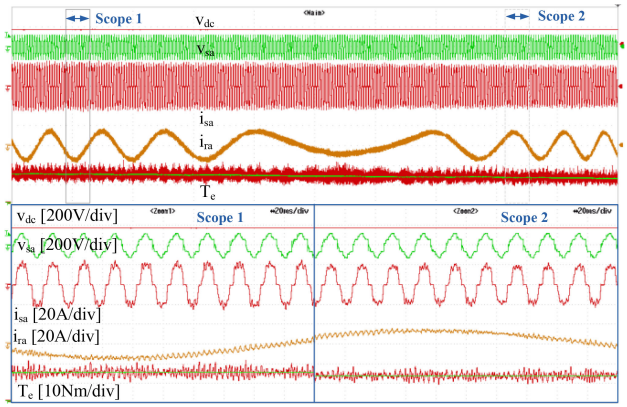

Fig. 19. Variable speed operation of DTI$_d$C controlled DFIG-DC.

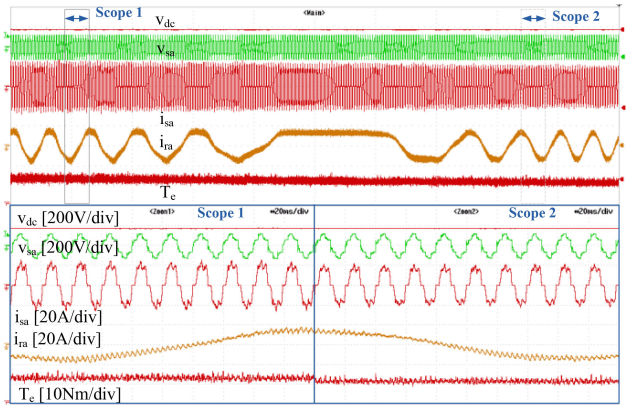

Fig. 20. Variable speed operation of DT|ψ|C controlled DFIG-DC.

X. Summary

This paper presents simulation and experimental results of comparison between three direct torque control methods and the field oriented control method for a stand-alone DFIG-DC voltage generator. Two of the proposed methods (DTI$_d$C, DTψ_dC) have open loop frequency control, and the DT|ψ|C method requires closed loop frequency control. The analyzed control methods were compared through simulation and experiments at the angle of torque oscillations reduction. The influence of the methods on generated instantaneous power p component oscillations responsible for DC bus voltage oscillations was discussed.

The laboratory test and simulations have shown that the largest torque pulsations were achieved in field oriented control. The direct torque control methods result in the smallest torque pulsations, and from among the three analyzed and tested methods the smallest torque pulsations have been achieved for direct torque control methods with flux controllers in the d control axis (DTψ_dC, DT|ψ|C).

The methods with open loop frequency control (both FOC and DTC) with an arbitrarily referenced variable in the d axis, entail slight phase shift between the reference frame orientation and the stator flux vector position. However, this displacement of the reference frame does not visibly influence the results.

APPENDIX

TABLE III
PARAMETERS OF THE 2MW SIMULATED DFIG-DC UNIT

PARAMETER	VALUE
Power	2MW
Stator voltage (L-L)	690 V
Rotor voltage (L-L)	2 kV
Number of pole pairs	2
L_m (Magnetizing inductance)	2.5 mH
L_s (Stator inductance)	2.587 mH
L_r (Rotor inductance)	2.587 mH
R_s (Stator resistance)	2.6 mΩ
R_r (Rotor resistance)	2.6 mΩ
f_s (Switching frequency)	4 kHz
C_{dc} (DC bus capacity)	10 mF

TABLE IV
PARAMETERS OF THE LABORATORY DFIG-DC UNIT

PARAMETER	VALUE
Power	7.5 kW
Stator voltage (L-L)	182 V
Rotor voltage (L-L)	380 V
Number of pole pairs	2
L_m (Magnetizing inductance)	27.52 mH
L_s (Stator inductance)	29.82 mH
L_r (Rotor inductance)	29.82 mH
R_s (Stator resistance)	0.16 Ω
R_r (Rotor resistance)	0.1 Ω
f_s (Switching frequency)	5 kHz
C_{dc} (DC bus capacity)	2 mF

REFERENCES

[1] V. Yaramasu, B. Wu, P. C. Sen, S. Kouro, and M. Narimani, "High-power wind energy conversion systems: State-of-the-art and emerging technologies," *Proc. IEEE*, vol. 103, no. 5, pp. 740–788, 2015.

[2] N. Yu, H. Nian, and Y. Quan, "A novel DC grid connected DFIG system with active power filter based on predictive current control," in *Proc. Int. Conf. Elect. Machines Syst.*, 2011, pp. 1–5.

[3] M. F. Iacchetti, G. D. Marques, and R. Perini, "Torque ripple reduction in a DFIG-DC system by resonant current controllers," *IEEE Trans. Power Electron.*, vol. 30, no. 8, pp. 4244–4254, Aug. 2015.

[4] G. D. Marques and M. F. Iacchetti, "A self-sensing stator-current-based control system of a DFIG connected to a DC-link," *IEEE Trans. Ind. Electron.*, vol. 62, no. 10, pp. 6140–6150, 2015.

[5] M. F. Iacchetti and G. D. Marques, "Voltage control in a DFIG-DC system connected to a stand-alone DC load," in *Proc. 9th Int. Conf. Compat. Power Electron.*, 2015, pp. 323–328.

[6] G. Abad, J. Lopez, M. Rodrıguez, L. Marroyo, and G. Iwanski, in *Doubly Fed Induction Machine - Modeling and Control for Wind Energy Generation*, IEEE Press Series on Power Engineering, Hoboken, NJ, USA: Wiley-IEEE Press, Dec. 2011.

[7] D. Forchetti, G. García, and M. I. Valla, "Vector control strategy for a doubly-fed stand-alone induction generator," in *Proc. 28th Annu. Conf. IEEE Ind. Electron. Soc.*, 2002, pp. 991–995.

[8] G. Iwanski and W. Koczara, "Sensorless direct voltage control of the stand-alone slip-ring induction generator," *IEEE Trans. Ind. Electron.*, vol. 54, no. 2, pp. 1237–1239, 2007.

[9] G. D. Marques and M. F. Iacchetti, "DFIG topologies for DC networks: a review on control and design features," *IEEE Trans. Power Electron.*, vol. 34, no. 2, pp. 1299–1316, 2019.

[10] M. R. A. Hamadi, A. Chandra, and B. Singh, "Hybrid AC-DC standalone system based on PV array and wind turbine," in *Proc 40th Annu. Conf. IEEE Ind. Electron. Soc.*, 2014, pp. 5533–5539.

[11] P. Maciejewski and G. Iwanski, "Direct torque control for autonomous doubly fed induction machine based DC generator," in *Proc. 12th Int. Conf. Ecolog. Veh. Renew. Energies.*, 2017, pp. 1–6.

[12] A. Gundavarapu, H. Misra, and A. K. Jain, "Direct torque control scheme for dc voltage regulation of the standalone DFIG-DC system," *IEEE Trans. Ind. Electron.*, vol. 64, no. 5, pp. 3502–3512, May 2017.

[13] N. Yu, H. Nian, and Y. Quan, "A novel DC grid connected DFIG system with active power filter based on predictive current control," in *Proc. Int. Conf. Elect. Machines Syst.*, 2011, pp. 1–5.

[14] I. Takahashi and T. Noguchi, "A new quick-response and high-efficiency control strategy of an induction motor," *IEEE Trans. Ind. Appl.*, vol. IA-22, no. 5, pp. 820–827, 1986.

[15] G. D. Marques and M. F. Iacchetti, "Minimization of torque ripple in the DFIG-DC system via predictive delay compensation," *IEEE Trans. Ind. Electron.*, vol. 65, no. 1, pp. 103–113, Jan. 2018.

[16] H. Misra, A. Gundavarapu, and A. K. Jain, "Control scheme for DC voltage regulation of stand-alone DFIG-DC system," *IEEE Trans. Ind. Electron.*, vol. 64, no. 4, pp. 2700–2708, Apr. 2017.

[17] A. Muhtadi and A. M. Saleque, "A performance study based on comparative analysis between SCIG and DFIG based wind energy conversion system in a microgrid at St. Martin's Island," in *Proc. 4th Int. Conf. Adv. Elect. Eng.*, 2017, pp. 439–444.

Paweł Maciejewski received the M.Sc. degree in automatic control and robotics, and the Ph.D. degree in electrical engineering from Faculty of Electrical Engineering at the Warsaw University of Technology (WUT), Warszawa, Poland, in 2012 and 2019, respectively. Since 2018 he has been an Assistant Professor in Institute of Control and Industrial Electronics WUT. He teaches courses on electric drives and energy conversion systems. His research interests include electric drives and generating systems with induction machines.

Grzegorz Iwanski (Senior Member, IEEE) received the M.Sc. degree in automatic control and robotics, and the Ph.D. degree in electrical engineering from Faculty of Electrical Engineering at the Warsaw University of Technology (WUT), Warszawa, Poland, in 2003 and 2005, respectively. Since January 2006 to December 2008 he was a Research Worker involved in international project within 6th Framework Programme of EU. Since 2009 he has been an Assistant Professor in Institute of Control and Industrial Electronics WUT; where in 2019 he received Associate Professor position. He teaches courses on power electronics, drives and power conversion systems. His research interests include variable and adjustable speed power generation systems, photovoltaic and energy storage systems, automotive power electronics and drives. In 2012/2013 he joined the team of REES UPC, Barcelona–Terrassa, within the framework of scholarship of Polish Minister of Science and Higher Education. He is co-author of one monograph, three books chapters, and about 70 journal and conference papers. He provided two plenary lectures on IEEE technically sponsored international conferences (EVER'15 and OPTIM-ACEMP'17).